Journal of the European Ceramic Society **16** (1996) 1107–1114

PII: S0955-2219(96)00038-6
0955-2219/96/$15.00

Indentation Fracture Toughness and Surface Flaw Analysis of Sintered Alumina/SiC Nanocomposites

C. C. Anya & S. G. Roberts*

University of Oxford, Department of Materials, Parks Road, Oxford OX1 3PH, UK

(Received 25 October 1995; revised version received 16 January 1996; accepted 23 January 1996)

Abstract

The fracture toughness (K_{Ic}) of pressureless-sintered monolithic α-alumina and its composites with 5, 10 and 15 vol% SiC nano-sized particles was investigated using Vickers indentation and a new Hertzian (ball) indentation technique. Both methods showed that the fracture toughness of the composites is better than that of alumina, although the results from the Vickers indentations were complicated by a change in crack geometry from median/radial (alumina) to Palmqvist (composites) An analysis of the number and size of surface flaws using the Hertzian test indicates that, for the same polishing treatment, the composites have a better surface finish. © 1996 Elsevier Science Limited.

Introduction

Small additions of nano-sized SiC particles to alumina (to produce 'nanocomposites') enhance its bend strength, compared with 'pure' alumina of the same grain size.[1,2] The mechanisms behind this enhancement of the mechanical properties remain unclear. Possible mechanisms could be:

(1) an increase in fracture toughness;
(2) a reduction in the number and size of processing-induced flaws; and
(3) an improved response to grinding and polishing, resulting in a reduction in the number and size of polishing-induced flaws.

While increases in strength as high as 186%[1] and 36%[2] have been reported for unannealed 5 vol% SiC–alumina composite (≥99.5% theoretical density), only modest increases in toughness have been reported. For instance, using the Vickers indentation technique, Zhao *et al.*[2] reported a maximum increase in K_{Ic} of 24% for this 5 vol% SiC–alumina 'nanocomposite'. (A similar sample, sintered to 98·2% of its theoretical density, showed a 7% reduction in K_{Ic}.[2])

* To whom correspondence should be addressed.

Use of Vickers indentation methods to determine fracture toughness can be problematic. Ponton and Rawlings[3] list 15 formulae for deriving K_{Ic} from measurements of surface crack lengths (c, measured as half the total crack span) around indentations made with a load P, in a material with Young's modulus E and hardness H, assuming that the crack geometry is of the 'median/radial' type. These are generally of the forms:

$$K_{Ic} = \alpha (E/H)^n (P/c^{3/2}) \quad (1)$$

or

$$K_{Ic} = \beta (P/c^{3/2}) \quad (2)$$

with varying pre-factors α and β depending on the assumptions that have been made about the indentation stress field, and n equal or close to 0·5. Given the very complex nature of deformation beneath a sharp indenter, especially in brittle materials, it is not easy to justify the choice of one variant of these formulae over the others, although versions where the hardness and elastic modulus of the material are included [eqn (1)] are probably preferable. Thus this method should be regarded with suspicion if *absolute* values for the fracture toughness are derived. Even if the Vickers indentation method is used simply for comparative studies of materials, the possibility that the crack geometry could change from one material to another should be considered. In eqns (1) and (2) the cracks are generally assumed to be 'half-penny' shaped (Fig. 1) — and this is not always, or even often, the case.[4] A further possibility is that the geometry of the crack may change more radically to the 'Palmqvist' type (Fig. 1), typically found in tougher ceramics such as WC–Co. Again, several formulae[3] have been produced relating K_{Ic} to crack length (l, the surface crack length on one side of the indentation), load P, and the indentation's semi-diagonal length a. They are generally of the form:

$$K_{Ic} = \gamma (E/H)^\delta P/(al^{1/2}) \quad (3)$$

In previous studies of the indentation fracture toughness of nanocomposites,[5] it has generally been assumed the indentation cracks are of the median/

radial type. In this study, we examine this assumption more closely by performing experiments to establish the actual crack shapes.

An alternative method for determining the fracture toughness of brittle materials has recently been established,[6] based on Hertzian indentation. Here a spherical indenter is used, so that the stress field under the indenter is well defined (unlike the case for the sharp indenter used in Vickers tests), and values of K_{Ic} in good agreement with values determined by four-point bend tests are obtained. The method makes use of a full analysis of the Hertzian contact field, in which it was found that even for a badly abraded surface, where a dense population of flaws of all sizes exists, there is always a minimum load needed to cause formation of the characteristic Hertzian 'ring crack'. This minimum load depends only on K_{Ic}, E and ν (Poisson's ratio) of the test material, and on the size of indenting ball used.

The Hertzian test can also be used to determine the size of the surface flaw which, in a given test, results in the formation of a ring crack. Analysis of many such tests (~20 or more) on a sample enables the density (number per unit surface area) of such flaws to be determined.[7]

This study investigates the fracture toughness of pressureless-sintered Al_2O_3–SiC composites by both Vickers and Hertzian indentation methods, and also uses the Hertzian tests to investigate the surface flaw sizes and densities in these materials.

Materials and Experimental Methods

The powders used were α-Al_2O_3 (AES 11c, Sumitomo) and α-SiC (UF-45, Lonza) with average particle sizes of 400 and 200 nm, respectively. Monolithic alumina and three composites with 5, 10 and 15 vol% SiC in an alumina matrix were fabricated. Powders were mixed by attrition milling, and then cold-isostatically pressed to 175 MPa. Materials were then pressureless-sintered at 1560°C for 2 h (alumina) and at 1775°C for 4 h (composites). The materials produced were found to be of ≥99·7% of their theoretical densities. The grain sizes of all materials were 3·5 ± 1·5 μm, though the alumina showed a bimodal grain structure. Full details of the preparation routes will be reported elsewhere.

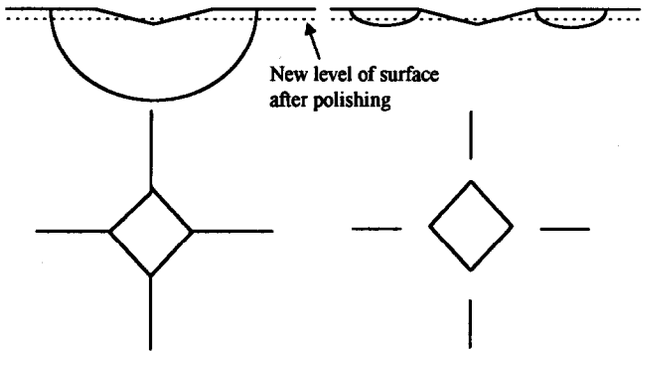

Fig. 1. Schematic representation of median/radial (left) and Palmqvist (right) crack systems. Upper diagrams show cross-sections of the crack systems below the surface, and lower diagrams plan views after polishing to the level shown. The crack trace becomes detached from the indentation for the Palmqvist system.

The Young's modulus E of the materials and their Poisson's ratios were determined by use of a 'Grindosonic' instrument (MK4i). Results are given in Table 1.

Samples of 6 mm thickness were cut from all four types of material using a diamond saw. They were all simultaneously ground and polished to a 3 μm finish. Vickers indentations were carried out at loads of 49, 98, 196 and 294 N. For each load at least five indentations were made, and the average indentation size and crack length parameters were used in analysis. To reduce any possible effects of environmentally assisted cracking, the measurements were always made within 2 h of indentation. Some indented samples were then polished to remove ~5 μm from the surface, to identify the crack geometry as either median/radial or Palmqvist. Analysis of fracture toughness based on these results is discussed later.

The Hertzian indentations were made with a 5 mm diameter alumina ball using a modified 'ET500' testing machine (Engineering Systems, Nottingham, UK). The loads at which ring cracks were formed were detected by acoustic emission. The loads were recorded, and the sizes of the matching ring cracks were measured by optical microscopy using Normarski differential interference contrast to enhance visibility of the ring cracks. Tests were performed on alumina, alumina–5% SiC and alumina–15% SiC composites. The test surfaces were finished with either 3 or 14 μm diamond paste. The 3 μm finish was used to compare the surface finishes produced by a 'good' polish on the various materials, while the 14 μm finish, with larger surface cracks, was used to determine K_{Ic}. Whereas the ring-cracks on the 3 μm polished composite could be observed without any further treatment, the cracks in the 14 μm ground samples required etching with KOH at 400°C, followed by light polishing with 3 μm diamond paste, to render the cracks visible. Ring cracks in monolithic alumina were made more visible by etching in KOH.

Results and Discussion

Vickers indentation

Crack paths

Table 1 gives a summary of the Vickers indentation results. Analysis of the results to give K_{Ic} requires knowledge of the crack type around the indentations.

One method[4] of doing this would be to fit the data of crack length to load: one would expect $c \propto P^{2/3}$ for median/radial cracks [eqns (1) and (2)] or $l \propto P^{1/2}$ for Palmqvist cracks [eqn (3)]. However, the data in Table 1 do not fit either relationship well; no conclusion can be drawn from these data about the active crack types.

Figure 2 shows the results of polishing away the surface of indented samples. The crack system in monolithic alumina is median/radial (cracks are continuous under the indentations), while that of all the composites is of Palmqvist type (cracks are separate wings on either side of the indentations). The continuity of the crack system across the indentation in

Table 1. Vickers indentation results

	Load (*N*)	*Diagonal* (*μm*)	*Crack length* (*μm*)	H *(conv.)* (*GPa*)	H *(Hamer)* (*GPa*)	K_{Ic} *(median)* ($\alpha = 0.016$) (*MPa* $m^{1/2}$)	K_{Ic} *(median)* ($\alpha = 0.022$) (*MPa* $m^{1/2}$)	K_{Ic} *(Palmqvist)* (*MPa* $m^{1/2}$)
Alumina	49·1	72·8 ± 0·5	106 ± 10	17·16 ± 0·24	18·51 ± 0·26	**2·14 ± 0·23**	3·06 ± 0·33	4·09 ± 0·28
	98·1	103 ± 2·0	167 ± 8	17·15 ± 0·69	18·49 ± 0·74	**2·25 ± 0·17**	3·22 ± 0·24	4·61 ± 0·30
E = 397·4 ± 3·0 GPa	196·2	150 ± 1·0	249 ± 11	16·17 ± 0·22	17·44 ± 0·23	**2·57 ± 0·15**	3·67 ± 0·22	5·31 ± 0·20
ν = 0·249	294·3	181 ± 1·4	299 ± 13	16·66 ± 0·26	17·97 ± 0·28	**2·88 ± 0·17**	4·11 ± 0·24	5·95 ± 0·24
5% SiC	49·1	69·6 ± 0·7	98 ± 12	18·78 ± 0·38	20·25 ± 041	2·28 ± 0·31	3·25 ± 0·44	**4·31 ± 0·39**
	98·1	99·2 ± 0·3	170 ± 6	18·49 ± 0·11	19·94 ± 0·12	2·16 ± 0·10	3·08 ± 0·15	**4·62 ± 0·13**
E = 399·5 ± 4·0 GPa	196·2	142·2 ± 0·4	260 ± 18	17·99 ± 0·10	19·41 ± 0·11	2·36 ± 0·20	3·38 ± 0·28	**5·26 ± 0·24**
ν = 0·254	294·3	176 ± 0·3	309 ± 30	17·62 ± 0·06	19·00 ± 0·06	2·73 ± 0·30	3·90 ± 0·43	**5·90 ± 0·35**
10% SiC	49·1	69·3 ± 1·00	90 ± 7	18·94 ± 0·56	20·43 ± 0·60	2·52 ± 0·24	3·60 ± 0·34	**4·53 ± 0·32**
	98·1	97 ± 0·5	140 ± 7	19·33 ± 0·20	20·85 ± 0·22	2·68 ± 0·16	3·83 ± 0·23	**5·15 ± 0·19**
E = 407·2 ± 2·0 GPa	196·2	135 ± 1·0	245 ± 15	19·96 ± 0·30	21·53 ± 0·32	2·47 ± 0·19	3·53 ± 0·27	**5·52 ± 0·27**
ν = 0·250	294·3	168 ± 0·5	338 ± 20	19·34 ± 0·12	20·85 ± 0·12	2·40 ± 0·17	3·43 ± 0·25	**5·74 ± 0·35**
15% SiC	49·1	65·8 ± 0·4	83 ± 5	21·01 ± 0·26	22·66 ± 0·28	2·67 ± 0·19	3·82 ± 0·27	**4·78 ± 0·22**
	98·1	95·5 ± 0	124 ± 14	19·95 ± 0·00	21·51 ± 0·00	3·04 ± 0·35	4·34 ± 0·50	**5·50 ± 0·36**
E = 409·5 ± 4·0 GPa	196·2	134 ± 2·0	235 ± 18	20·26 ± 0·62	21·85 ± 0·67	2·59 ± 0·26	3·70 ± 0·37	**5·66 ± 0·42**
ν = 0·237	294·30	163 ± 1·0	308 ± 40	20·54 ± 0·25	22·15 ± 0·27	2·63 ± 0·30	3·76 ± 0·55	**6·06 ± 0·54**

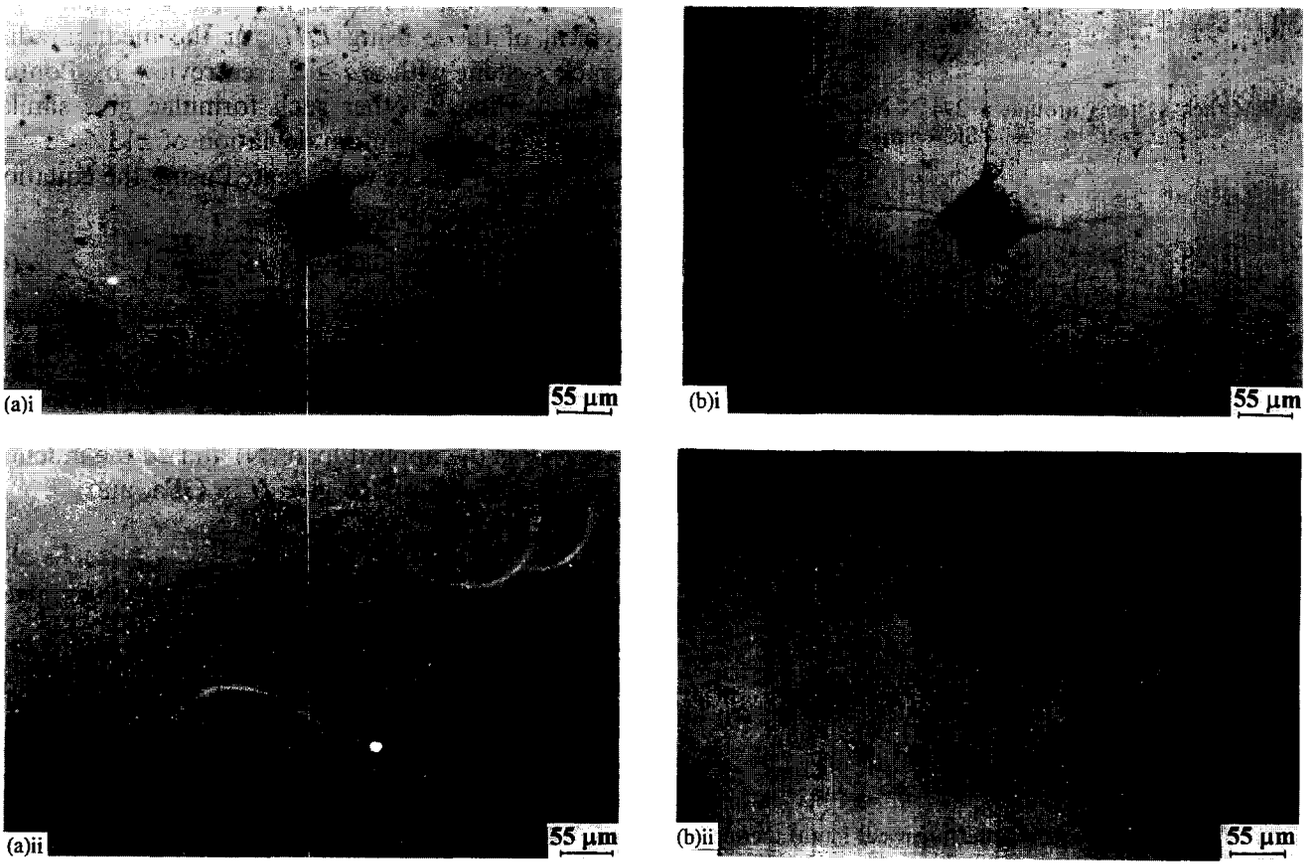

Fig. 2. Crack systems of materials around 98 N Vickers indentations: (a) as indented — (i) alumina, (ii) 5 vol% SiC composite; (b) polished after indentation — (i) alumina, (ii) 5 vol% SiC composite. The 10% and 15% composites are similar to the 5 vol% SiC composite.

the monolithic alumina has a tendency to encourage grain fall-out in these indentations. It has been suggested[8,9] that Palmqvist cracks at lower loads could evolve into median types at higher loads. This was not the case in this study. Figure 3 shows surfaces polished after indentation with 294 N load for alumina [median/radial type cracking, Fig. 3(a)] and 5 vol% SiC composite [Palmqvist type, Fig. 3(b)].

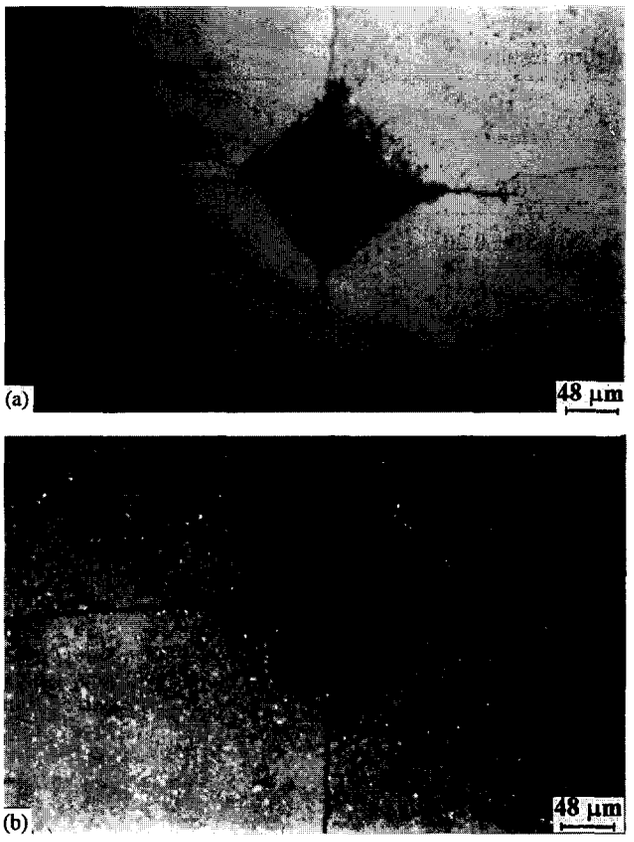

Fig. 3. Crack systems around a 294 N Vickers indent: (a) alumina; (b) 5 vol% SiC composite.

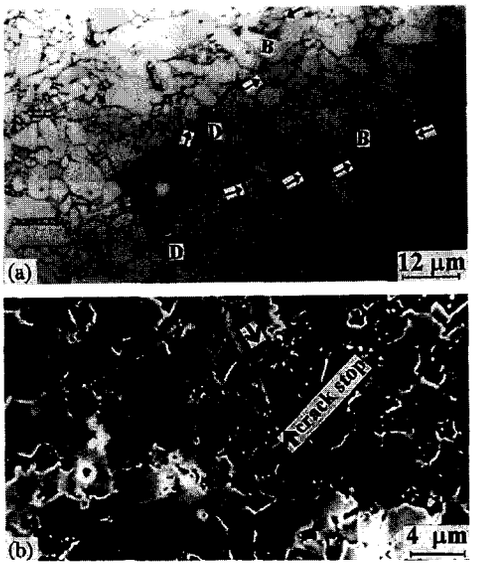

Fig. 4. Micrographs of crack paths (arrowed) in: (a) thermally etched Al_2O_3 (optical image); (b) chemically etched 5% SiC composite (scanning electron image). Note the intergranular nature of the path in alumina [with bridge (B) and deflection (D) positions marked] and the transgranular path in the composite.

The crack paths are predominantly intergranular for alumina [Fig. 4(a)] with bridges (for example, B) and deflections (D), whereas in the composites [Fig. 4(b)] cracks are principally transgranular. This possibly indicates a strengthening of the grain boundaries relative to those in monolithic alumina. This difference in crack paths has been observed by other workers.[10]

Determination of K_{Ic} *values*

Table 1 shows K_{Ic} values determined for the materials tested. The formula used for median/radial cracks was the equation proposed by Anstis *et al.*[11]

$$K_{Ic} = 0{\cdot}016(E/H)^{1/2}(P/c^{3/2}) \quad (4)$$

The table also shows K_{Ic} determined in this manner but with a deformation field geometry constant of 0·022:

$$K_{Ic} = 0{\cdot}022(E/H)^{1/2}(P/c^{3/2}) \quad (5)$$

Equation (5) was used so as to compare our results directly with those obtained for sintered 5 vol% SiC nano-composite by Zhao *et al.*[2] They used eqn (5) in order 'to compensate for the effects of environmentally assisted crack growth' (although they did not show that this had occurred). However, since we measured crack lengths soon after indentation, any such effect should be minimal. Equation (4) is typical of those using E/H, for the median/radial crack system with $c/a \geq 2$ (see review by Ponton and Rawlings[3]); other such formulae give similar results with a maximum deviation of ±13%.

Palmqvist cracks were treated using the equation proposed by Niihara *et al.*:[12]

$$K_{Ic} = 0{\cdot}0089(E/H)^{2/5}(al^{1/2}) \quad (6)$$

Hardness values were calculated with the standard equation:

$$H = 1854{\cdot}4P/(2a)^2 \quad (7)$$

where P is the applied load (N) and $2a$ the indentation diagonal (μm), to give H in GPa, and

$$H = 1000P/2a^2 \quad (8)$$

for direct comparison with hardness values given using this equation by Zhao *et al.*[2]

Vickers indentation K_{Ic} *results*

Table 1 shows that SiC additions appear to improve the toughness of alumina with the greatest change being between monolithic alumina and alumina–15% SiC. However, these differences depend on using the equations appropriate to the crack geometries seen (values given in bold in the table); the differences disappear if the same equation is used for all

materials. Given the uncertainties in the numerical pre-factors in equations such as (4)–(6), due to the poorly defined indentation stress fields, the results from this type of test must thus be regarded with extreme caution.

For a given material, the calculated fracture toughness increases with increasing load and thus crack size, as shown in Fig. 5(a). Such increases may be due to a number of effects, e.g. crack bridging and friction in the crack wake, or effects of residual stresses. If the effect is due solely to an internal stress field (as will arise from the thermal expansion mismatch of the SiC particles in the Al_2O_3 matrix), one might, by analogy with effects seen in transformation-toughened zirconia,[13] expect the toughness to increase linearly with the square root of the crack size. That is not, however, the case for our materials [see Fig. 5(b)]; any direct effects of residual stresses on K_{Ic} appear to be less important than other possible '*R*-curve' mechanisms.

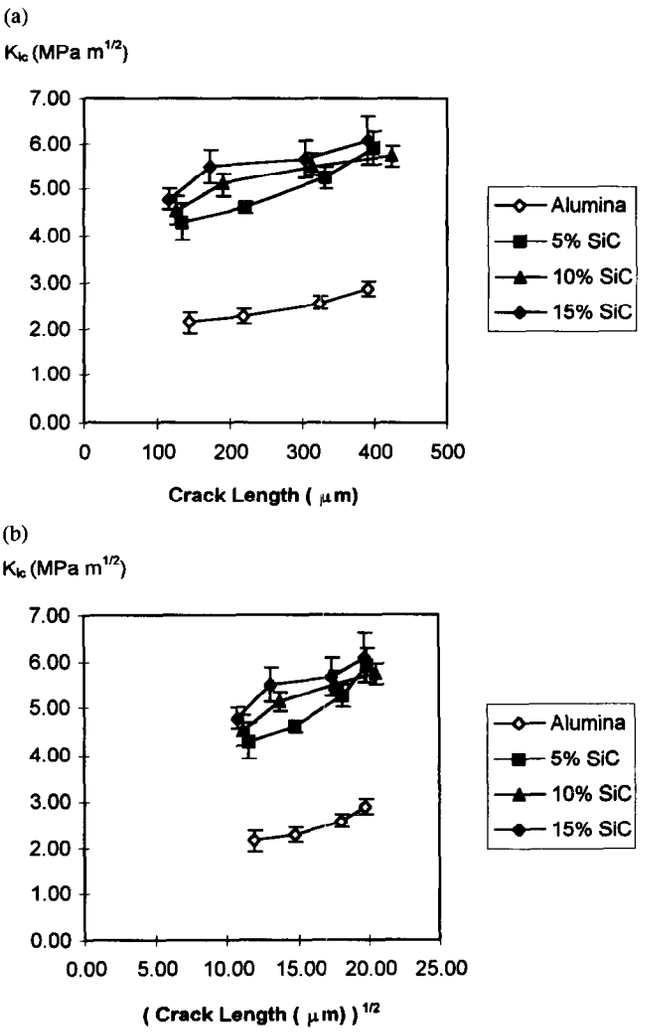

Fig. 5. Vickers indentation toughness K_{Ic} as a function of: (a) crack length; (b) square root of crack length.

Since the Vickers indentation methods for determining K_{Ic} in these materials gave ambivalent results, highly dependent on the formulae used, another method for determining K_{Ic} was used. This method is based on Hertzian indentation.

Hertzian indentation

Fracture toughness

Recent analyses of the stress intensity acting on cracks in the Hertzian stress field (that due to the elastic contact between a sphere and a flat surface, or between two spheres) have led to a new technique for determining the fracture toughness of brittle materials.[6] The near-surface radial stresses of the Hertzian field are tensile only very close to the surface, and rapidly become compressive with depth. The stresses also decay rapidly away from the contact area. Detailed analysis shows that there is a *minimum* load at which a surface flaw can propagate into the characteristic Hertzian 'ring/cone' crack, even if the surface is densely populated with flaws of all sizes and orientations. This minimum load depends only on the elastic moduli of the ball and surface and the fracture toughness of the surface (for cases where the ball and surface have the same elastic moduli; if they are dissimilar, then frictional tractions also must be taken into account). The method has been shown to give accurate values for K_{Ic}, compared with four-point bend measurements, for alumina and glass.[6]

Tests are performed by indenting a moderately abraded surface (to give a high density of surface flaws, so that one corresponding to the minimum load for fracture is likely to be found near a given indentation). The fracture toughness K_{Ic} may be calculated with the formula[6]

$$K_{Ic} = [(E^* P_{Fmin})/CR]^{1/2} \quad (9)$$

$$E^* = E/2(1 - \nu^2) \quad (9a)$$

where P_{Fmin} is the minimum fracture load in all tests, C is a constant depending only on the Poisson's

Table 2. Fracture toughness measured by Hertzian indentation

	Surface finish			
	3 μm diamond		*14 μm diamond*	
Material	$P_{Fmin}(N)$	$K_{Ic}(MPa\ m^{1/2})$	$P_{Fmin}(N)$	$K_{Ic}(MPa\ m^{1/2})$
Al_2O_3	330 ± 9	2·9 ± 0·1	335 ± 9	2·9 ± 0·1
Al_2O_3–5% SiC	465 ± 5	3·6 ± 0·1	511 ± 14	3·7 ± 0·1
Al_2O_3–15% SiC	520 ± 15	4·0 ± 0·1	590 ± 30	4·3 ± 0·1

ratio ν of the material being tested, E is its Young's modulus and R is the radius of the spherical indenter (polycrystalline Al_2O_3).

Values of K_{Ic} obtained are shown in Table 2. The values obtained with the two different surface finishes are reasonably consistent. The results are also consistent with the trends in the values obtained from the Vickers indentation tests, if the differences in crack geometry between the alumina and the composite samples are taken into account. We are thus confident that the fracture toughness of the composites is genuinely higher than that of pure alumina of the same grain size.

Flaw statistics

Figure 6 shows the cumulative probability of ring-crack formation with increasing load in a Hertzian test for the alumina and a 5% SiC composite. The fracture loads for the composite are ~80% higher than those for alumina. Since the fracture toughness values of the materials vary only by ~40%, this indicates that the surface flaws from which fracture originates are smaller in the composite material, although all materials received the same nominal surface finish. By measuring the ring-crack size for each test, it is possible to calculate the depth of the original surface flaw from which the ring crack originated.[7]

Figure 7 shows the results of such analysis on samples finished with 14 μm diamond [Fig. 7(a)] and 3 μm diamond [Fig. 7(b)], as histograms of the fraction of surface flaws found in a given size range. The majority of the surface flaws for the composites finished with 14 μm diamond are in the 3·5–5·5 μm size range, while for the alumina, flaws of all sizes up to 13 μm deep were found. It was not possible to measure ring-crack sizes on 3 μm finished alumina samples, but the nanocomposites finished to this level of polish showed a tighter distribution of flaws than those finished with 14 μm diamond.

Further analysis of the results gives the area density of surface flaws in a given size range, using a development by Warren *et al.*[7] of Wilshaw's 'searched area' method.[14] The new analysis takes into account the variation with depth of the Hertzian

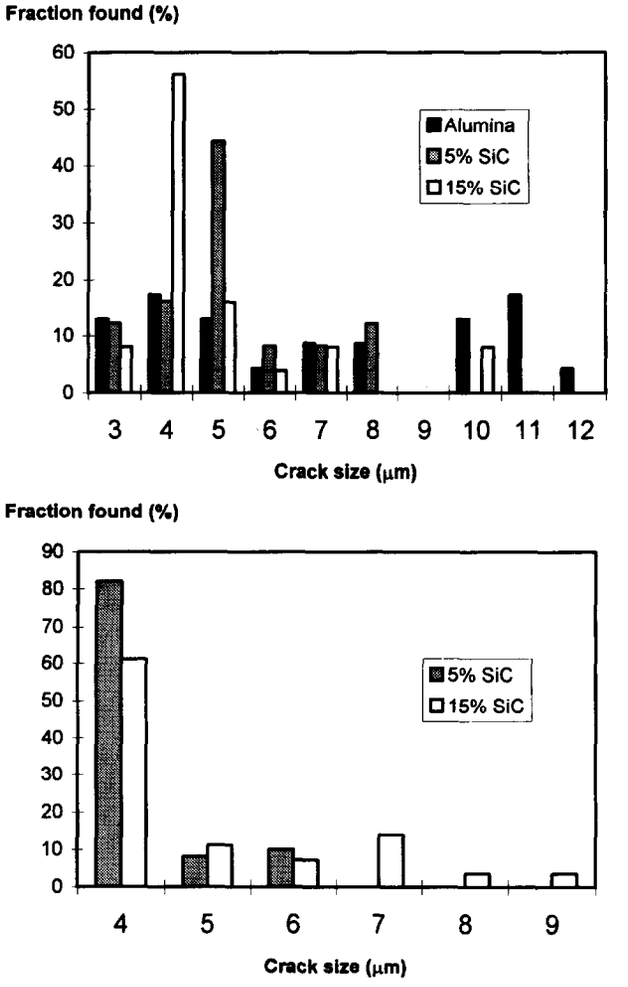

Fig. 7. Flaw statistics on samples finished with (a) 14 μm diamond and (b) 3 μm diamond, as histograms of the fraction of surface flaws in a 1 μm size range centred about the value shown.

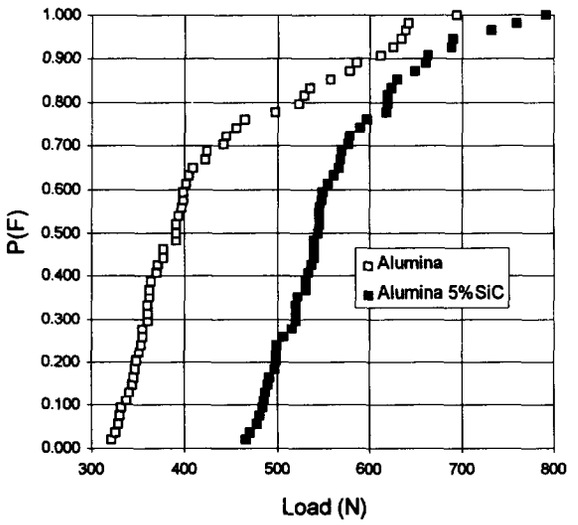

Fig. 6. Cumulative probability of failure $P(F)$ versus Hertzian indentation fracture loads for the monolithic alumina and the 5% SiC composite, both finished with 3 μm diamond paste.

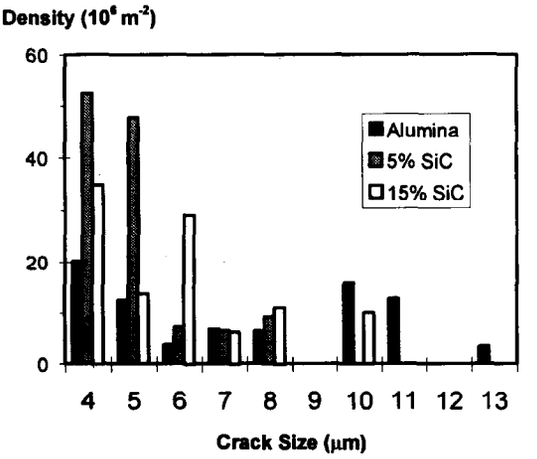

Fig. 8. Flaw statistics on samples finished with 14 μm diamond, as area density of surface flaws in a 1 μm size range centred about the crack depth shown.

stress field and all possible orientations of surface flaws. Results for the 14 μm polished specimens are shown in Fig. 8. As expected from Fig. 6, the composites have a much higher density of small surface flaws compared with the alumina, which has a significant density of large flaws.

Typical ring cracks are shown in Fig. 9(a) for alumina and Figs 9(b) and (c) for the 5 vol% SiC composite. It can be seen that the rings are not as well formed in alumina as in the composite. Note also the large number of grain pull-outs in the alumina surface compared with the composite; this may be either a result of, or a cause of, the large flaws found on the alumina surfaces.

A common method of analysing data similar to those in Fig. 6 is to perform a 'Weibull analysis', assuming that the probability of failure $P(F)$ varies with stress σ, and area (volume) tested A, as:

$$1 - P(F) = \exp\left[-\frac{A}{A_0}\left(\frac{\sigma}{\sigma_0}\right)^m\right] \qquad (10)$$

where σ_0 is a normalizing stress and A_0 is a normalizing load. For simple cases (e.g. bend tests, tensile tests), the stress and stress intensity on a flaw rises linearly with applied load (L) in the test. In this case, plotting $\ln\{\ln[1/(1-P(F))]\}$ against $\ln(L)$ yields a straight line with gradient m. Figure 10 shows such plots for the data of Fig. 6. It is immediately apparent that a straight line does not result. This is because of the complexity of the stress field around a Hertzian indenter, which has two effects on the assumptions of the Weibull analysis:

(1) the stress intensity on a given flaw does not rise linearly with applied load, especially for larger flaws; and
(2) the area 'searched' for a flaw of a given size is not the whole specimen, but depends in a complex way on the loads applied in the whole series of tests.

Warren[15] has analysed a simplified case of the effects of Hertzian indentation on a surface with a flaw distribution where the flaw density $\rho(c)$ for a given flaw size, c, is given by:

$$\rho(c) = A\, c^{-r} \qquad (11)$$

where r is a constant. In this case, for small flaws (i.e. those that are totally contained within the tensile surface stress), a relationship exists between the slope on a 'Hertzian Weibull' plot (such as Fig. 10), m_H and the normal Weibull modulus, m:

$$m = 3m_H - 2 = 2(r - 1) \qquad (12)$$

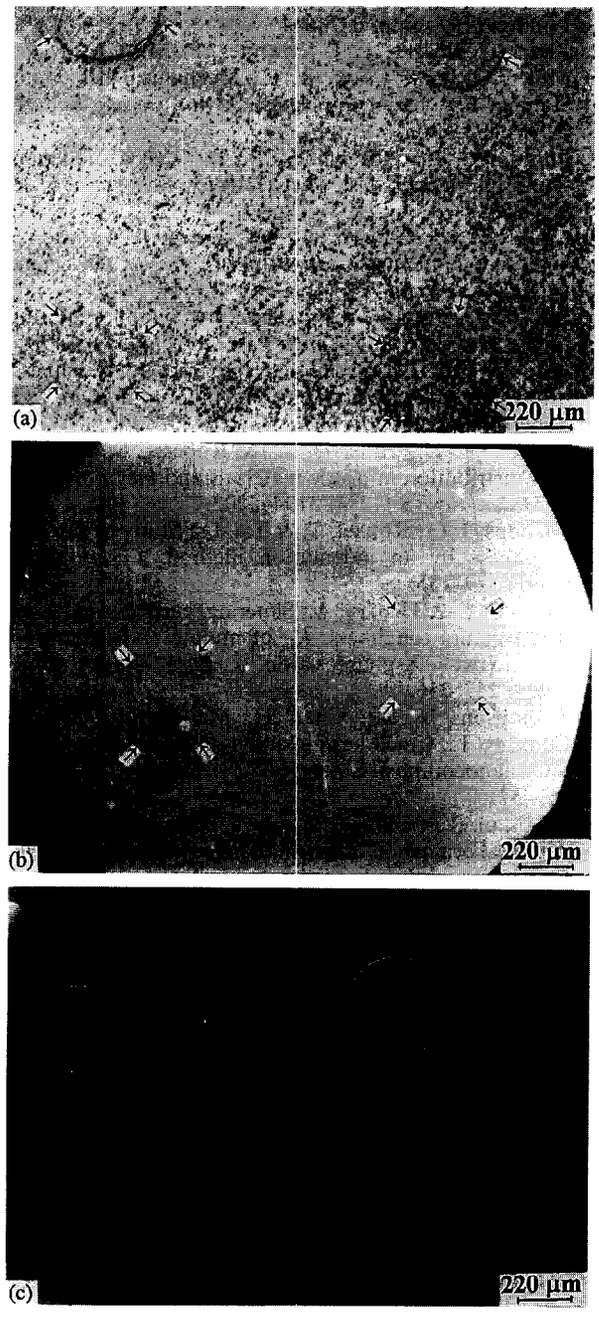

Fig. 9. Ring cracks from Hertzian indentations: (a) alumina, ground to 14 μm finish; (b) 5 vol% SiC composite, ground to 14 μm finish; (c) 5 vol% SiC composite, ground to 3 μm finish. The rings, or segments, are arrowed for clarity.

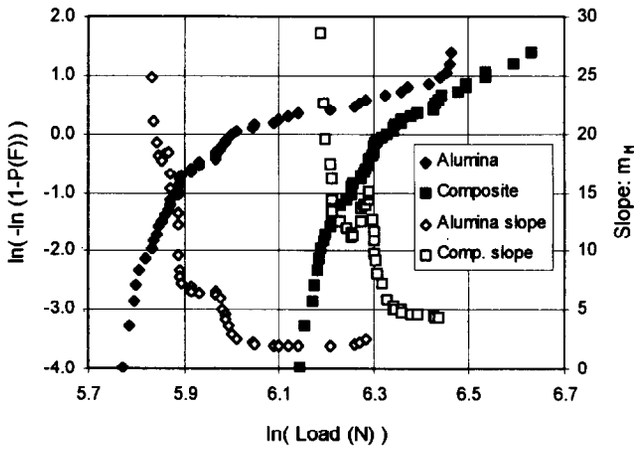

Fig. 10. 'Weibull plot' of data from Fig. 6. Note the non-linearity of the plots, especially in the low fracture load (i.e. large flaw) regime. The local slopes, m_H, of the lines are calculated as 'floating' linear regressions of 20 points centred around the load shown.

The 'small flaw' region on Fig. 10 corresponds to the highest fracture loads, where indeed the gradient is very nearly constant. Values of m derived from Fig. 10 are: alumina, $m \approx 4$ (i.e. $m_H \approx 2$); alumina 5% SiC, $m \approx 10$ (i.e. $m_H \approx 4$). However, our data only give information about the 'small flaw' end of the complete flaw distribution; flaws in this size range are not those likely to cause failure in bending or tension. The Weibull moduli thus derived may not, therefore, apply directly to the relative tensile reliability of these materials.

Conclusions

The results given in detail above may be summarized as follows.

(1) Indentation of sintered monolithic alumina produces a median/radial crack geometry, while indentation of its composites with up to 15 vol% SiC particles produces Palmqvist cracks.

(2) Calculation of Vickers indentation fracture toughness using formulae appropriate to the crack types gives K_{Ic} values of ~2·0–3·0 MPa $m^{1/2}$ for the alumina and ~4·5–6·0 MPa $m^{1/2}$ for the composites.

(3) The Vickers indentation K_{Ic} of all the materials tested increases with crack length (higher loads) — a behaviour similar to that of materials with an 'R-curve' characteristic.

(4) Hertzian indentation gives K_{Ic} values of 2·9 MPa $m^{1/2}$ for the alumina and ~3·5–4·0 MPa $m^{1/2}$ for the composites. The Hertzian method deals with the extension of cracks in the 1 to 10 μm range, so the differences between these results and those from the Vickers indentations may be a reflection of the different crack sizes operative in the two techniques.

(5) Identical polishing treatments produce different surface finishes on the alumina and the composites. The composites have flaw distributions centred around a smaller flaw size, and with a tighter distribution, compared with the alumina. Larger flaws in alumina seem to be associated with grain pull-out, which is almost totally suppressed in the composites.

Future papers will report on the strength and wear resistance of these materials.

Acknowledgements

This project was funded by the EPSRC (Grant No. GR/J/77542). We thank Cookson plc for use of the Isopress and furnace facilities. We thank Dr R. W. Davidge and Dr B. Derby for discussion of the results. We are grateful to Dr P. D. Warren for discussions of the Hertzian indentation methods, and for provision of computer programs to process the data.

References

1. Niihara, K. & Nakahira, A., Particulate strengthened oxide nanocomposites. In *Advanced Structural Inorganic Composites*, ed. Vincenzini. Elsevier Science Publishers, London (1990), pp. 637–664.
2. Zhao, J., Stearns, L. C., Harmer, P. M., Chan, H. M., Miller, G. A. & Cook, R. F., Mechanical behaviour of alumina–SiC 'nanocomposites'. *J. Am. Ceram. Soc.*, **76**[2] (1993) 503–510.
3. Ponton, C. B. & Rawlings, R. D., Vickers indentation fracture toughness test: Part 1. *Mater. Sci. Tech.*, **5** (1989) 865–872.
4. Cook, R. F. & Pharr, G. M., Direct observation and analysis of indentation cracking in glasses and ceramics. *J. Am. Ceram. Soc.*, **73**[4] (1990) 787–817.
5. Sakai, M. & Bradt, R. C., Fracture toughness testing of brittle materials. *Int. Mater. Rev.*, **38**[2] (1993) 53–78.
6. Warren, P. D., Determining the fracture toughness of brittle materials by Hertzian indentation. *J. Eur. Ceram. Soc.*, **15**[3] (1995) 201–207.
7. Warren, P. D., Hills, D. A. & Roberts, S. G., Surface flaw distribution in brittle materials and Hertzian fracture. *J. Mater. Res.*, **9** (1994) 3194–3202.
8. Glandus, J. C., Rouxel, T. & Tai, Q., Study of the Y-TZP toughness by an indentation method. *Ceram. Int.*, **17** (1991) 129–135.
9. Anya, C. C. & Hendry, A., Sintering, hardness and indentation fracture toughness, K_{Ic} of mullite and its composite with 15 wt% X-phase sialon. *J. Euro. Ceram. Soc.*, **13** (1994) 247–256.
10. Thompson, A. M., Chan H. M., Harmer, M. P. & Cook, R. F., Crack healing and stress relaxation in Al_2O_3–SiC 'nanocomposites'. *J. Am. Ceram. Soc.*, **78**[3] (1995) 567–571.
11. Anstis, G. R., Chantikul, P., Lawn, B. R. & Marshall, D. B., A critical evaluation of indentation techniques for measuring fracture toughness by direct crack measurements. *J. Am. Ceram. Soc.*, **64**[9] (1981) 533–538.
12. Niihara, K., Morena, R. & Hasselman, D. P. H., Evaluation of K_{Ic} of brittle solids by the indentation method with low crack-to-indent-ratios. *J. Mater. Sci. Lett.*, **1** (1982) 13–16.
13. Ikuma, Y. & Virkar, A. V., Crack-size dependence of fracture toughness in transformation-toughened ceramics. *J. Mater. Sci.*, **19** (1984) 2233–2238.
14. Wilshaw, T. R., The Hertzian fracture test. *J. Phys. D: Appl. Phys.*, **4** (1971) 1567–1581.
15. Warren, P. D., Private communication.